Modeling and Experimental Studies of Emulsion Copolymerization Systems. III. Acrylics

ENRIQUE SALDÍVAR,[1] ODAIR ARAUJO,[2] REINALDO GIUDICI,[3] CARLOS GUERRERO-SÁNCHEZ[1]

[1] CID-GIRSA, Av. Sauces 87 Mza.6 Lerma México

[2] Rhodia S. A., Usina Química de Paulínia, 13140-000, SP Brasil

[3] Dept. de Engenharia Química, Universidade de São Paulo, 05424-970, SP, Brasil

Received 27 September 2000; accepted 6 March 2001

ABSTRACT: Using a previously published model and continuing the series of papers started with styrenic copolymers, predictions for evolution of conversion and average particle diameter in batch experiments are compared against experimental data for four emulsion copolymerizations involving at least one acrylic monomer: (1) methyl methacrylate/butyl acrylate, (2) methyl methacrylate/butadiene, (3) methyl methacrylate–vinyl acetate, and (4) butyl acrylate/vinyl acetate. For each system a fraction of factorial experiments were run covering simultaneous variations in five variables: initiator [*I*] and surfactant [*E*] concentrations, water to monomer ratio (*W*/*M*), monomer composition, and temperature. Data fitting is performed to represent the experimental data as several parameters are not available from independent experimental sources. The model is able to explain the effects of simultaneous changes in emulsifier concentration, initiator concentration, and water to monomer ratio on conversion and average particle size histories, although in some cases only qualitatively. An assessment of the degree in which a general emulsion copolymerization model is useful for practical applications is made. Physical insight is also gained by observing the trends of adjusted parameters with temperature and copolymer composition. © 2002 Wiley Periodicals, Inc. J Appl Polym Sci 84: 1320–1338, 2002; DOI 10.1002/app.10003

Key words: emulsion copolymerization; mathematical modeling

INTRODUCTION

The first part of this series of papers included experimental results for a number of copolymer systems produced by emulsion polymerization. In the second part, more detailed experimental results and comparison with model simulations were presented for the styrenic copolymerization systems studied. In this third part the focus is on experimental data and simulations for the acrylic systems, specifically methyl methacrylate/butyl acrylate, methyl methacrylate/butadiene, methyl methacrylate/vinyl acetate, and butyl acrylate/vinyl acetate.

This is the first work published in which an extensive set of data for several emulsion copolymerization systems is used to assess the applicability of a general mathematical model in terms of its ability to fit and explain experimental data of conversion, particle size, and copolymer composition. The task of modeling with some generality this type of systems is formidable, due to the complexity of emulsion copolymerization and the peculiarities of each specific pair of monomers.

Correspondence to: E. Saldívar (esaldiva@mail.girsa.com.mx).

Contract grant sponsors: CID-GIRSA, CNPq, and FAPESP.

Journal of Applied Polymer Science, Vol. 84, 1320–1338 (2002)

Parameter fitting of unknown and uncertain parameters of the model is unavoidable in order to fit large sets of data; however, physical insight can be gained by a judicious analysis of trends observed in the adjusted parameters.

In the modeling philosophy adopted in this work all parameters for which reliable values are available are taken from the literature. Unknown or uncertain parameters are fitted to experimental data restricting the adjusted parameter values to lie between physically reasonable limits. Using this approach both: the theoretical plausibility of the model as well as its practical applicability can be assessed. See paper 2 of this series[1] for an extended discussion on this issue.

In this work, following the approach of the previous paper of this series, the experimental data of Araujo[2] for four emulsion copolymerizations of acrylic systems are discussed and contrasted with a mathematical model[1,3,4] predictions. Again, two goals are pursued: (1) to gain insight in the mechanisms governing emulsion copolymerization rate of reaction for acrylic systems and (2) to assess the quantitative degree of understanding of emulsion copolymerization. Hopefully, this work will encourage the use of mathematical modeling in industrial applications of emulsion copolymerization and will help clarify in which specific areas of emulsion copolymerization theory there is a need for more research.

In the following section a literature review of previous work on emulsion copolymerization of acrylic systems is done. In the third section of the paper the experiments performed on the systems methyl methacrylate/butyl acrylate, methyl methacrylate/butadiene, methyl methacrylate/vinyl acetate, and butyl acrylate/vinyl acetate are presented. For a summary of the mathematical model of Saldívar et al.,[3,4] the reader is referred to the second paper of this series.[1] In Results and Discussion, the copolymerization systems are simulated with the mathematical model, and simulation predictions are discussed and compared with experimental data.

PREVIOUS WORK

Acrylic polymers and copolymers are very important systems from the industrial point of view. When produced in emulsion, they are used in high quality coatings and paints. The increased polarity of acrylic monomers, as compared to that of styrene, makes them an interesting subject of study from the scientific standpoint. Still, very few comparative studies have been published in which the copolymerization of acrylic monomers with several monomers is considered.

Methyl methacrylate/butyl acrylate (MMA/BA) emulsion copolymerization has been studied by several researchers focusing on kinetic and particle structure aspects,[5–12] soapless emulsion polymerization,[13,14] and semicontinuous processes.[15–17] Emelie et al.[5,6] studied the influence of emulsifier and initiator concentration and monomer to water ratio on the polymerization rate. Urretabizkaia et al.[7] monitored conversion and copolymer composition by calorimetric measurements: they also applied their technique to the emulsion copolymerizations of methyl methacrylate/vinyl acetate and butyl acrylate/vinyl acetate. As part of a systematic study on the kinetics of multicomponent polymerization, Dube and Penlidis[8] ran a 50/50 molar emulsion copolymerization of the MMA/BA system. They observed a rather constant rate of polymerization during the reaction with evidence for the presence of gel effect. Barton et al.[10] studied the kinetics of polymerization of MMA over seed particles of poly(butyl acrylate). A number of papers discuss core–shell emulsion copolymerization of BA/MMA with a core rich in BA and a shell rich in MMA.[11–14] A practical application of this polymer is the toughening of poly(methyl methacrylate).[12] Presumably, the production of emulsifier-free core–shell BA/MMA particles could be used to reinforce clear poly(methyl methacrylate) without affecting its optical properties. Working with a soapless system, Pan et al.[13] studied the effect of monomer composition on the final properties of the copolymer. They found evidence of phase separation in the particles ending up with a copolymer containing a BA-rich phase in the core and an MMA-rich phase in the shell. Lee et al.[14] deliberately produced core (BA)–shell (MMA) copolymers by a two-stage soapless process. Unzueta and Forcada[15,16] studied the effect of emulsifier type on the particle number in seeded and unseeded semicontinuous emulsion copolymerization of MMA/BA. Chern and Hsu[17] studied the effect of emulsifier concentration and other variables on the particle size distribution (PSD) for this emulsion copolymerization. The driving force for the studies just mentioned[15–17] seems to be the importance of the PSD on coating and paint applications of latex of MMA/BA.

As opposed to the previous system, the emulsion copolymerization of methyl methacrylate/butadiene (MMA/B) has received very little attention in the literature. To the authors knowledge,

Table I Experimental Design: Methyl Methacrylate/Butyl Acrylate System

Run	Temperature	MMA Level	[*I*]	[*E*]	*M*/*W*
1	+	−	−	−	−
2	+	+	−	−	−
4	−	+	−	−	−
5	+	−	+	+	−
6	+	+	+	−	−
7	−	−	+	−	−
8	−	+	+	+	−
9	−	−	−	−	−
12	−	+	−	+	−
13	+	+	−	−	+

Temperature: [+] = 70°C, [−] = 60°C; %MMA/%BA: [+] = 70/30, [−] = 30/70; [*I*]: [+] = 0.004 mol/L-aq, [−] = 0.002 mol/L-aq; [*E*]: [+] = 0.028 mol/L-aq, [−] = 0.014 mol/L-aq; monomer to water ratio (wt): [+] = 0.55, [−] = 0.34.

Table III Experimental Design: Methyl Methacrylate/Vinyl Acetate System

Run	Temperature	MMA Level	[*I*]	[*E*]	*M*/*W*
1	+	−	−	−	−
2	+	+	−	−	−
4	−	+	−	−	−
6	+	+	+	−	−
7	−	−	+	−	−
8	−	+	+	+	−
9	−	−	−	−	−
11	−	−	−	+	+
12	−	+	−	+	−
13	+	+	−	−	+

Temperature: [+] = 70°C, [−] = 60°C; %MMA/%VA: [+] = 70/30, [−] = 30/70; [*I*]: [+] = 0.004 mol/L-aq, [−] = 0.002 mol/L-aq; [*E*]: [+] = 0.028 mol/L-aq, [−] = 0.014 mol/L-aq; monomer to water ratio (wt): [+] = 0.55, [−] = 0.34.

only the work by Shapiro et al.[18] has focused on this system to study the effect of the emulsifier on the copolymer microstructure. No much work has been reported on copolymerization of MMA and B using other type of processes, either. A few works have studied the synthesis of block copolymers of MMA/B via anionic polymerization.[19–21]

Methyl methacrylate/vinyl acetate (MMA/VA) emulsion copolymerization has also received scarce attention in the literature. Canegallo et al.[22] used on-line densimetry in order to measure conversion during the reaction. Saldívar and Ray[23] studied the control of copolymer properties in semicontinuous emulsion copolymerization; they selected this system due to the large difference in copolymerization reactivity ratios between the two monomers. The kinetics of this copolymerization in bulk and in solution has been studied by a few authors.[24,25]

The emulsion copolymerization of butyl acrylate/vinyl acetate (BA/VA) has been studied by several authors. Composition and composition control through semicontinuous processes has been the subject of several works.[26–33] Other studies have addressed the influence of polymerization variables on the filming properties and other physicochemical properties of the latex of

Table II Experimental Design: Methyl Methacrylate/Butadiene System

Run	Temperature	MMA Level	[*I*]	[*E*]	*M*/*W*
1	+	+	−	−	−
2	+	−	−	−	−
5	+	+	+	+	−
6	+	−	+	−	−
9	−	+	−	−	−
14	+	−	+	+	−
15	+	+	−	+	−
16	++	+	−	−	−
17	++	−	−	−	−
18	++	−	−	+	−

Temperature: [++] = 80°C, [+] = 70°C, [−] = 60°C; %MMA/%B: [+] = 70/30, [−] = 30/70; [*I*]: [+] = 0.004 mol/L-aq, [−] = 0.002 mol/L-aq; [*E*]: [+] = 0.028 mol/L-aq, [−] = 0.014 mol/L-aq; monomer to water ratio (wt): [−] = 0.34.

Table IV Experimental Design: Vinyl Acetate/Butyl Acrylate System

Run	Temperature	VA Level	[*I*]	[*E*]	*M*/*W*
1	+	−	−	−	−
2	+	+	−	−	−
3	−	−	−	+	−
4	−	+	−	−	−
5	+	−	+	+	−
6	+	+	+	−	−
7	−	−	+	−	−
9	−	−	−	−	−
10	−	+	−	−	+
12	−	+	−	+	−
13	+	+	−	−	+

Temperature: [+] = 70°C, [−] = 60°C; %VA/%BA: [+] = 70/30, [−] = 30/70; [*I*]: [+] = 0.004 mol/L-aq, [−] = 0.002 mol/L-aq; [*E*]: [+] = 0.028 mol/L-aq; [−] = 0.014 mol/L-aq; monomer to water ratio (wt): [+] = 0.55, [−] = 0.34.

Table V Gel Effect and Termination Correlations

Methyl Methacrylate
$V_{fi} = A_0 + A_1 (T_K - A_2)$
$V_{fpi} = A_0 + A_3 (T_K - A_4)$
$V_f = \phi_{p1} V_{f1} + \phi_{p2} V_{f2} + \phi_{pp} V_{f1} \Sigma_{i=1}^{c} \Phi_{pi} V_{fpi}$
$g_{p1} = 1$ for $V_f > A_5$
$g_{p1} = A_6 \exp(A_7 V_f)$ for $V_f < A_5$
$V_{fc} = A_8 - A_9 T_c$
$g_{t1} = A_{10} \exp(A_{11} V_f - A_{12} T_c)$ for $V_f > V_{fc}$
$g_{t1} = A_{13} \exp(A_{14} V_f)$ for $V_f \leq V_{fc}$
Copolymerization Termination and Propagation Constants
$g_p = g_{p1}^{\Phi_{p1}} g_{p2}^{\Phi_{p2}}$
$g_f = (g_{t1} g_{t2})^{1/2}$
$k_{tii} = g_t k_{t0ii}$
$k_{pii} = g_p k_{p0ii}$
$k_{t12} = k_{t21} = \phi (k_{t11} k_{t22})^{1/2}$
$k_{tr12} = k_{tr21} = \phi (k_{tr11} k_{tr22})^{1/2}$
$k_{pij} = k_{pij}/r_i$

x = total conversion, T_K = temperature in °K, T_c = temperature in °C, V_{fi} = free volume of component i, V_{fpi} = free volume of homopolymer i, ϕ_{pi} = volume fraction of component i in particles, Φ_{pi} = mass fraction of component i in copolymer, r_i = copolymer reactivity ratio for monomer i.

BA/VA.[34–38] Delgado et al.[39] compared the processes of miniemulsion and traditional emulsion copolymerization for this pair of monomers. The structure and morphology of the particles formed in the emulsion copolymerization of this system has also been studied.[40–43] Jourdan et al.[40] and Kong et al.[41] have confirmed that in batch processes a core–shell type structure is formed with a BA-rich core and a VA-rich shell. Other works have focused on kinetic aspects of this copolymerization, especially on the evaluation of apparent reactivity ratios.[44,45]

Table VI Values of Parameters Fitted for Runs 1, 5, 2, 6, and 13 of System Methyl Methacrylate/Butyl Acrylate (70°C)

	Value		
Parameter	30/70	70/30	Units
$k_{m_m} = k_{m_p}$	7×10^{-6}	5×10^{-5}	m/s
a_{em}	1.8×10^{-18}	1×10^{-17}	m^2
$D_{eff,1} D_{eff,2}$	5×10^{-12}	1×10^{-14}	m^2/s
Gel effect, A_5	3.5×10^{-2}	1.5×10^{-2}	L
Gel effect, A_6	4.8×10^{-6}	5.2×10^{-3}	

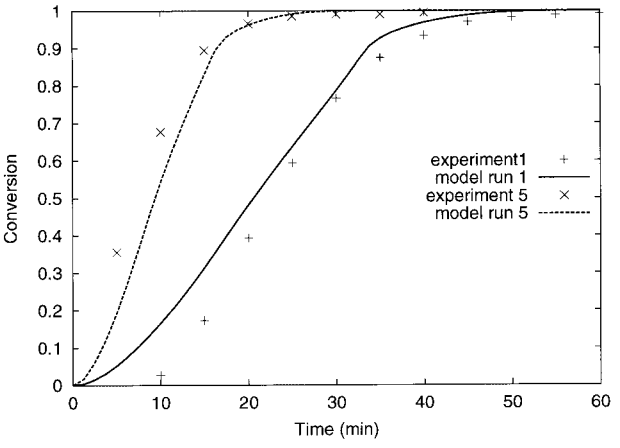

Figure 1 Model and experimental conversion–time curves for the MMA/BA system, runs 1 and 5.

EXPERIMENTAL

The experimental procedure followed during the polymerizations is given elsewhere[1,46] as well as the complete experimental design performed. In this section, only those parts of the experimental design that were simulated and analyzed with the mathematical model are presented in Tables I–IV. The reasons why some of the designed experiments were left out of the analysis are as follows: (1) it was not possible to run the experiment; (2) the experiment was run but there were experimental difficulties that rendered the data not reliable; (3) the experiment was run in conditions very different from the rest of the experimental design, so the comparison with other experiments was not very useful.

Measured responses were conversion by gravimetry, average particle diameter by photon correlation spectroscopy (dynamic light scattering), and copolymer composition by ^{1}H NMR. In this paper only the particle diameter and conversion data are simulated and discussed. Copolymer composition results were discussed before.[46]

RESULTS AND DISCUSSION

The kinetic scheme and a summary of the model for general emulsion copolymerization used in this work is given in the second paper of this series.[1] As mentioned in that paper, this is a simplified version of the complete model of Saldívar et al.[4] In this simplified version all the complex reaction steps, such as transfer to polymer, transfer to terminal and to internal double bonds,

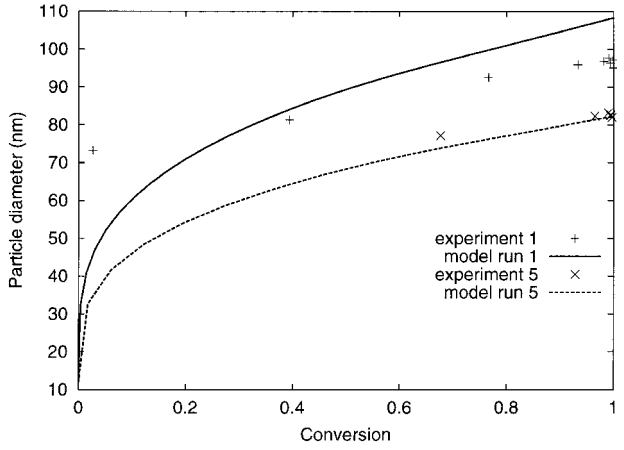

Figure 2 Model and experimental average particle diameter–conversion curves for the MMA/BA system, runs 1 and 5.

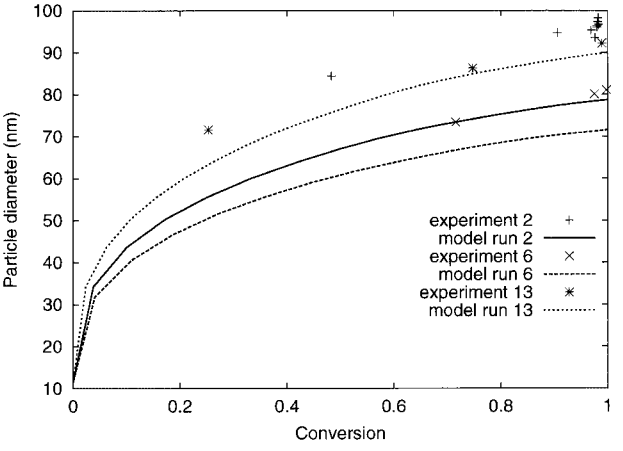

Figure 4 Model and experimental average particle diameter–conversion curves for the MMA/BA system, runs 2, 6, and 13.

etc., are not taken into account. These reaction steps can be ignored since they directly affect only the molecular weight distribution (MWD), and it is assumed that the kinetics and the PSD are not influenced by the MWD. For the simulations in this work further simplification came from the fact that only those steps corresponding to reactions present in the system were turned on. The model used is flexible enough to allow one to turn on or off a specific reaction step, so only those steps regarded as necessary were included. Steps not included were chain transfer to the chain transfer agent (CTA) (since no CTA was added), inhibition, redox initiation, and reverse propagation. The reader can also identify which specific steps were included by looking at the values of kinetic rate constants contained in the parameter tables of the main body of the paper and of the appendixes; those nonzero values correspond to kinetic steps included in the calculations. Also for the gel effect, the reader can identify for which systems its calculation was turned on by looking at the parameter value tables. As before, the solution of the model implemented in the POLYRED software package was used. Details on the solution of the model are given elsewhere.[3]

The simulations were performed by obtaining from the literature reported values for as many model parameters as possible. For those parameters of the model not available in the literature, data were adjusted using conversion–time and particle size–conversion data. The general parameters used for fitting the data for acrylic systems were the critical micelle concentration

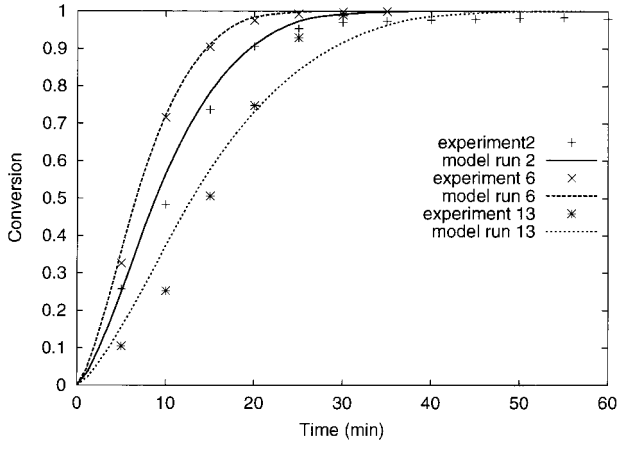

Figure 3 Model and experimental conversion–time curves for the MMA/BA system, runs 2, 6, and 13.

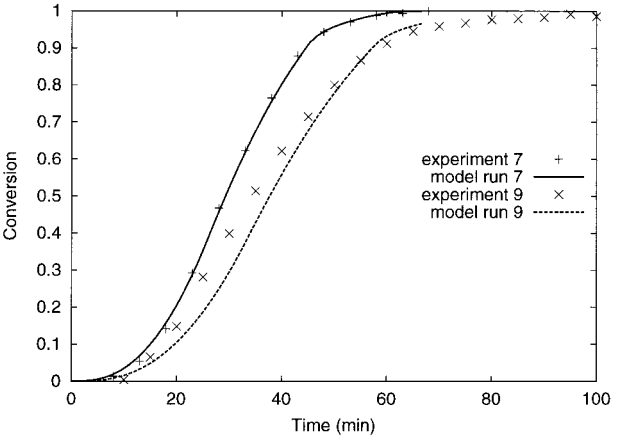

Figure 5 Model and experimental conversion–time curves for the MMA/BA system, runs 7 and 9.

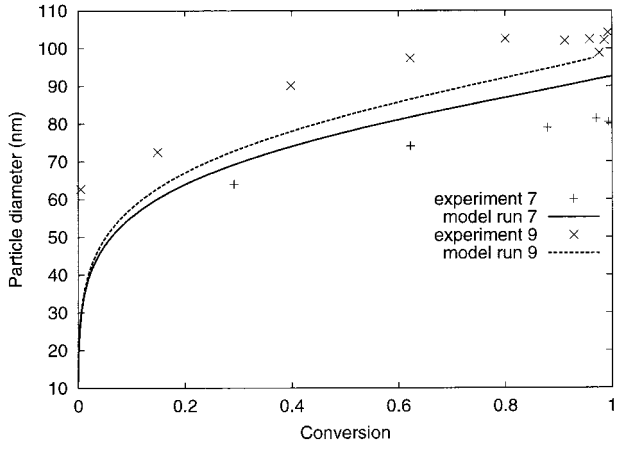

Figure 6 Model and experimental average particle diameter–conversion curves for the MMA/BA system, runs 7 and 9.

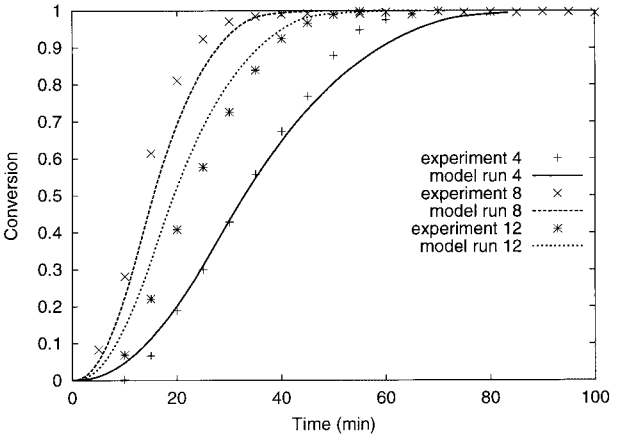

Figure 7 Model and experimental conversion–time curves for the MMA/BA system, runs 4, 8 and 12.

(CMC) of the emulsifier, the entry rate coefficients, and an effective diffusion coefficient for desorption of monomeric radicals from the particle. This is the same set of adjustable parameters used for data fitting of the styrenic systems reported before[3]; the selection of these parameters was also previously discussed. Only in the case of MMA/VA data, which posed special difficulties to fit, the radius of the micelle was also used as an additional adjustable parameter.

The form of the individual gel effect correlations for methyl methacrylate was taken from Schmidt and Ray[47]; the form of termination correlations for the copolymerization system was taken from Saldívar et al.[4] The gel effect was included for all the systems containing MMA and introduced through values for g_{pMMA} and g_{tMMA} calculated as shown in Table V, as well as values of $g_{\mathrm{p2}} = g_{\mathrm{t2}} = 1$ for the second monomer. No gel effect was included for the system VA/BA since VA polymerization shows a mild gel effect and no reliable data for BA polymerization gel effect could be found in the literature.

As in the previous paper, effective values D_{eff} for diffusion coefficients of the monomeric radicals were used; these effective values are defined as

$$\frac{D_{\mathrm{eff},i}}{3} = \frac{D_{\mathrm{w}i} D_{\mathrm{p}i}}{m_{\mathrm{d}i} D_{\mathrm{p}i} + 2D_{\mathrm{w}i}} \tag{1}$$

Composition-dependent effective diffusion coefficients were used as adjustable parameters to fit experimental data.

System Methyl Methacrylate/Butyl Acrylate

It was found that some of the parameters in the adjustable set required variable values depending on reaction temperature and on monomer composition in the feed, but the model was used with a fixed set of parameter values for simultaneous changes in emulsifier concentration, initiator concentration, and monomer to water ratio. For reactions at 70°C, one set of parameter values was used for the data at 30/70 MMA/BA molar composition (runs 1 and 5). Out of this set, some parameter values were changed to fit the data with high (70%) MMA composition (runs 2, 6, and 13). All values are listed in Table VI. Figures 1–4 show the comparison of experimental data and model predictions for conversion—time and average particle size—conversion for 70°C data. Also

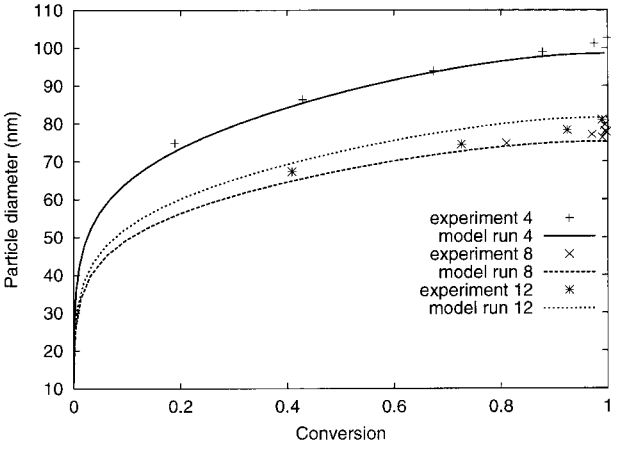

Figure 8 Model and experimental average particle diameter–conversion curves for the MMA/BA system, runs 4, 8, and 12.

Table VII Values of Parameters Fitted for Runs 7, 9, 4, 8, and 12 of System Methyl Methacrylate/Butyl Acrylate (60°C)

Parameter	Value 30/70	Value 70/30	Units
$k_{m_m} = k_{m_p}$	3.3×10^{-7}	4.6×10^{-7}	m/s
a_{em}	2.9×10^{-17}	1.8×10^{-17}	m^2
$D_{eff,1}$	1×10^{-9}	1×10^{-10}	m^2/s
$D_{eff,2}$	3×10^{-11}	2×10^{-13}	m^2/s
Gel effect, A_5	2.5×10^{-2}	1×10^{-2}	L
Gel effect, A_6	1.6×10^{-4}	3×10^{-2}	

for reactions run at 60°C the data were divided into two groups: those with a 30/70 MMA/BA molar composition (runs 7 and 9) and those with a 70/30 MMA/BA composition (runs 4, 8, and 12). Experimental data and simulation results are shown in Figures 5–8 and the values of adjusted parameters are given in Table VII. Parameters that required variable values to fit the four subsets were the micellar area covered by a surfactant molecule, a_{em}, effective diffusion coefficients, entry rate coefficients, and glass effect parameters. As mentioned in the previous paper of this series and elsewhere,[48] parameter a_{em} of the surfactant may depend on the copolymer composition. With respect to effective diffusion coefficients, from parameter fitting results, they tend to decrease with an increase in temperature and a decrease in MMA. A decrease in effective diffusion coefficients with an increase in temperature was only observed for systems containing butyl acrylate (BA) (see also the discussion for the VA/BA system). A possible explanation for this phenomenon is the promotion of gel formation

Table VIII Values of Parameters Fitted for Runs 1, 5, 15, and 2, 6, 14 of System Methyl Methacrylate/Butadiene (70°C)

Parameter	Value 30/70	Value 70/30	Units
$k_{m_m} = k_{m_p}$	4.8×10^{-7}	4×10^{-7}	m/s
a_{em}	2.5×10^{-18}	8×10^{-18}	m^2
CMC	3×10^{-3}	8×10^{-4}	gmol/L
$D_{eff,1}$	9×10^{-10}	2×10^{-11}	m^2/s
$D_{eff,2}$	9×10^{-9}	2×10^{-11}	m^2/s
Gel effect, A_5	4×10^{-2}	1.5×10^{-2}	L
Gel effect, A_6	8.3×10^{-7}	5.2×10^{-3}	

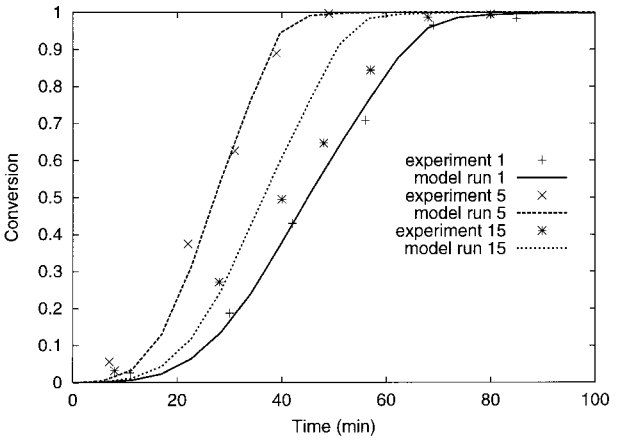

Figure 9 Model and experimental conversion–time curves for the MMA/B system, runs 1, 5, and 15.

due to transfer to polymer reactions caused by the presence of BA,[49] together with the fact that these reactions are also promoted with high temperatures[50] (if due to hydrogen abstraction, for example). High contents of gel may lead to hindered diffusion, making the effective diffusion coefficients decrease. This hypothesis is supported by the fact that in this investigation the presence of gel was higher for systems containing BA.[46] On the other hand, for constant temperature, lower values of effective diffusion coefficients with lower content of MMA could be a consequence of the larger solubility of MMA in the aqueous phase. This effect is implicit in eq. (1) through the parameter m_{di}, which is the partition coefficient of monomeric radicals between particles and aqueous phase.[4,51]

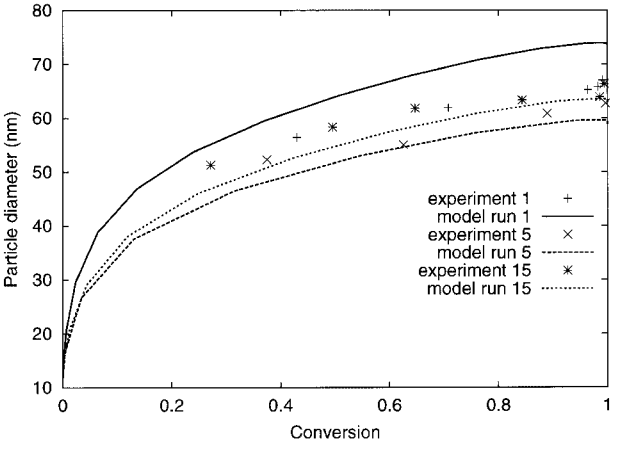

Figure 10 Model and experimental average particle diameter– conversion curves for the MMA/B system, runs 1, 5, and 15.

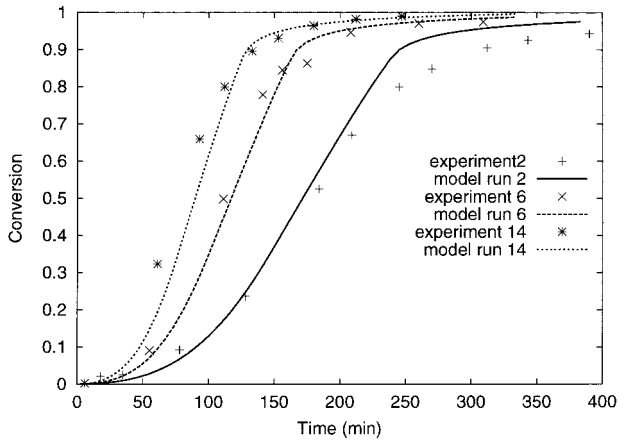

Figure 11 Model and experimental conversion–time curves for the MMA/B system, runs 2, 6, and 14.

With respect to the A_5 glass effect parameter, the higher the temperature and the content of butyl acrylate, the larger its value. This parameter represents a critical value for the free volume of the reaction media in the particles; below this value of free volume, diffusion limitations become the controlling factor for propagation. Lower values of A_5 mean that diffusion limitations for propagation are triggered at lower conversions. A_5 dependence on temperature and monomer composition could be explained using similar arguments to those used to explain the effect of these variables on effective diffusion coefficients.

In some cases the model tends to underestimate the effects of process variable changes on particle size and/or conversion. This is especially noticeable in the prediction of particle size for runs 7 and 9 (Fig. 6). These two runs differ only in the initiator concentration. See below the general discussion on model lack of fit for particle size data.

Table IX Values of Parameters Fitted for Runs 16, 17, and 18 of System Methyl Methacrylate/ Butadiene (80°C)

Parameter	Value 30/70	Value 70/30	Units
$k_{m_m} = k_{m_p}$	8×10^{-7}	3.7×10^{-6}	m/s
a_{em}	2×10^{-18}	4×10^{-18}	m^2
CMC	3×10^{-3}	8×10^{-3}	gmol/L
$D_{eff,1}D_{eff,2}$	2×10^{-9}	9×10^{-10}	m^2/s
Gel effect, A_5	5.2×10^{-2}	3.3×10^{-2}	L
Gel effect, A_6	1.2×10^{-8}	9.6×10^{-6}	

System Methyl Methacrylate/Butadiene

Runs 1, 5, 15, and 2, 6, and 14, were all performed at 70°C. Monomer molar ratios were 70/30 MMA/B for runs 1, 5, and 15, and 30/70 MMA/B for runs 2, 6, and 14. Values of fitted parameters are given in Table VIII. Comparison of experimental and model-predicted curves for conversion–time and average particle size–conversion is made in Figures 9–12.

For experiments run at 80°C, two sets of data were assembled for analysis. Run 16, having a 70/30 MMA/B composition, is the only experiment in the first set and the other set is formed by runs 17 and 18 with a 30/70 MMA/B composition. The values of the parameters fitted are given in Table

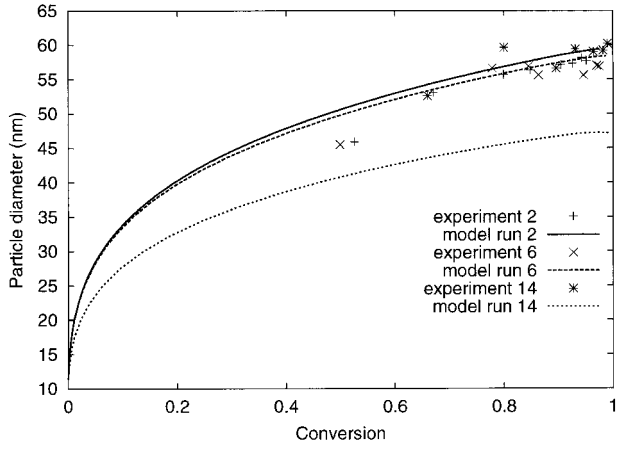

Figure 12 Model and experimental average particle diameter– conversion curves for the MMA/B system, runs 2, 6, and 14.

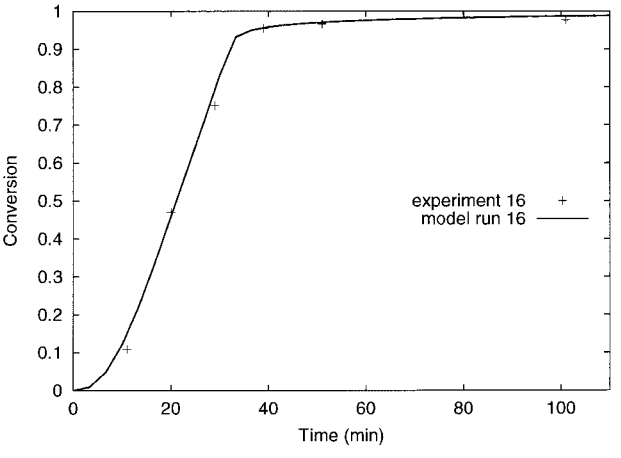

Figure 13 Model and experimental conversion–time curve for the MMA/B system, run 16.

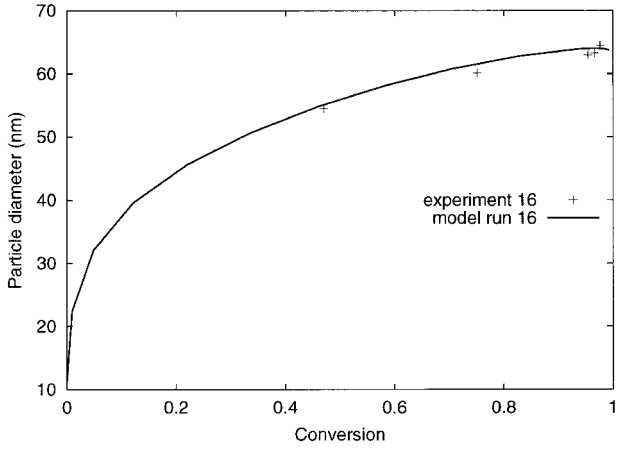

Figure 14 Model and experimental average particle diameter– conversion curve for the MMA/B system, run 16.

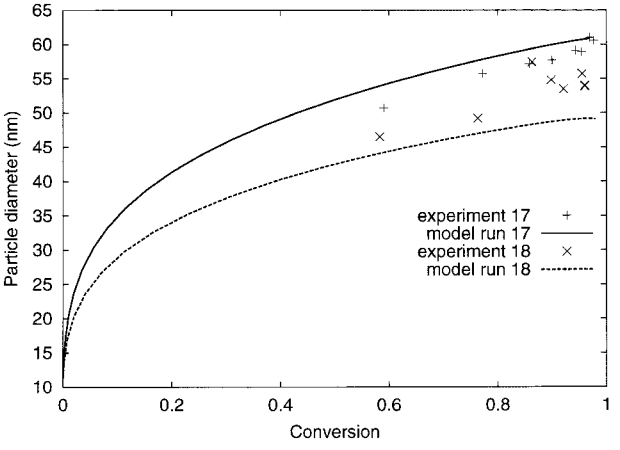

Figure 16 Model and experimental average particle diameter–conversion curves for the MMA/B system, runs 17 and 18.

IX. Results of simulations and experiments for runs at 80°C are shown in Figures 13–16. One run, experiment 9, was performed at 60°C with a 70/30 MMA/B composition; parameter values fitted for this run are given in Table X, and experimental and modeling curves are shown in Figures 17 and 18.

By comparing the parameter values in Tables VIII–X, the following generalizations can be made:

- entry rate coefficients increase with temperature;
- surface area covered by a surfactant molecule decreases with temperature and with increased butadiene content;
- glass effect parameter A_5 increases with temperature;
- effective diffusion coefficients increase with butadiene content.

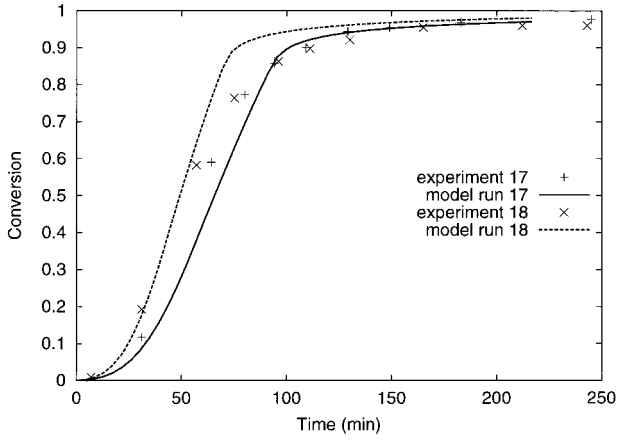

Figure 15 Model and experimental conversion–time curves for the MMA/B system, runs 17 and 18.

Temperature has a mixed effect on effective diffusion coefficients. On one hand, higher temperatures directly favor larger diffusivities; on the other hand, higher temperatures accelerate branching reactions of butadiene, which lead to gel formation and possible hindered diffusion if a desorbing radical is generated in a densely crosslinked local region. This may explain the fact that effective diffusion coefficients do not exhibit any clear trend with temperature. This is different from the case of butyl acrylate copolymers in which there seems to be a stronger trend of hindered diffusion at higher temperatures of reaction; however, it is noteworthy that butadiene copolymers show the presence of gel in lesser extent than butyl acrylate copolymers.

With respect to model agreement with experimental data, similar to other copolymer systems

Table X Values of Parameters Fitted for Run 9 of System Methyl Methacrylate/Butadiene (60°C)

Parameter	Value 70/30	Units
$k_{m_m} = k_{m_p}$	3.5×10^{-7}	m/s
a_{em}	2×10^{-17}	m^2
$D_{eff,1}D_{eff,2}$	4×10^{-11}	m^2/s
Gel effect, A_5	1.5×10^{-2}	L
Gel effect, A_6	5.2×10^{-3}	

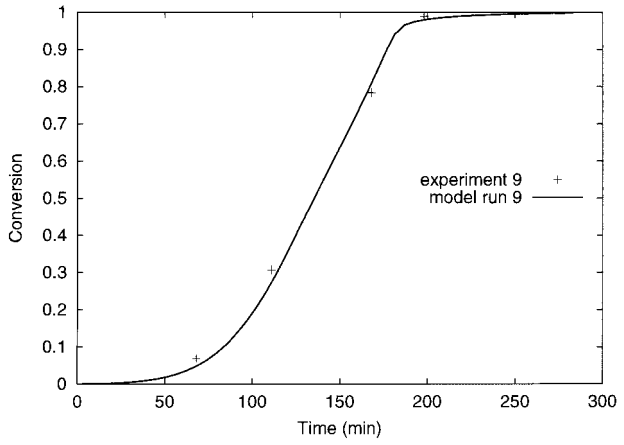

Figure 17 Model and experimental conversion–time curve for the MMA/B system, run 9.

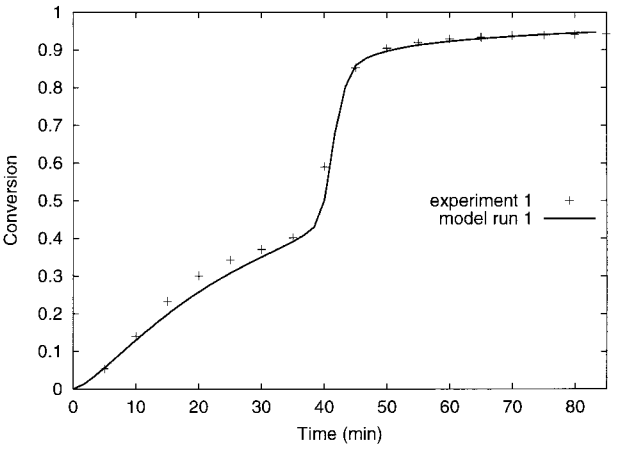

Figure 19 Model and experimental conversion–time curves for the MMA/VA system, run 1.

analyzed in this work, the evolution of particle diameter is described only in a semiquantitative way. Experimental particle size evolution data for runs 1, 5, and 15 are hardly distinguishable (Fig. 10), especially for runs 1 and 15, which differ only in the emulsifier concentration. Model predicted differences are more pronounced. A similar situation occurs for runs 2, 6, and 14, although for this set experimental data were available mostly at high (>60%) conversions (Fig. 12). The possible reasons for lack of fit of model predictions for particle size data are discussed below for all the systems together.

Conversion–time curve for run 18 shows significant model lack-of-fit above 60% conversion (Fig. 15). After that conversion the experimental data seem to show a decay in reaction rate that is not explained by the model, although the experimental data below 8 % conversion are too few (4) to draw any conclusion.

System Methyl Methacrylate/Vinyl Acetate

For experiment 1, run at 70°C, model and experimental curves are shown in Figures 19 and 20 for conversion evolution and for average particle size–conversion. For runs 2, 6, and 13, plots are shown in Figures 21 and 22. Fitted parameters are given in Table XI for all the data at 70°C.

Data from experiments run at 60°C were also grouped in two sets for analysis: (1) runs 7, 9, and 11 with a 30/70 (MMA/VA) molar ratio; and (2) runs 4, 8, and 12 with a 70/30 (MMA/VA) molar ratio. Figures 23–25 contain experimental results

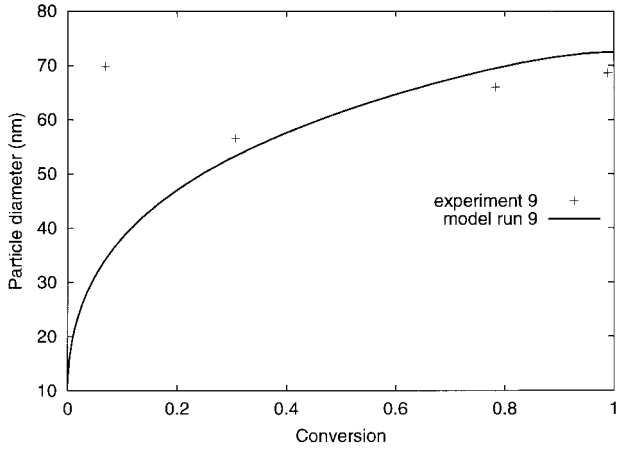

Figure 18 Model and experimental average particle diameter–conversion curve for the MMA/B system, run 9.

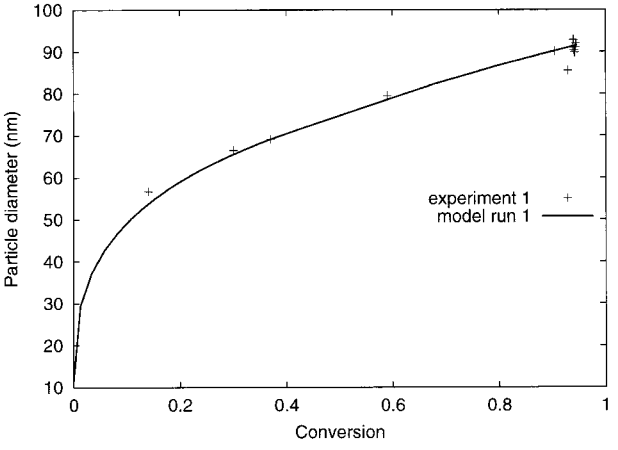

Figure 20 Model and experimental average particle diameter–conversion curves for the MMA/VA system, run 1.

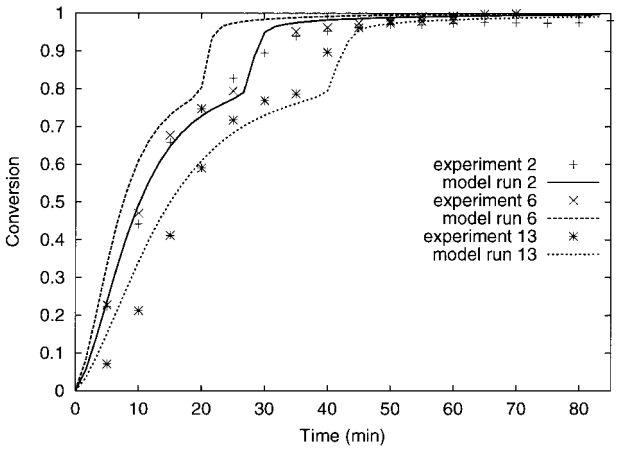

Figure 21 Model and experimental conversion–time curves for the MMA/VA system, runs 2, 6, and 13.

and model simulations for these runs. Adjusted parameters are included in Table XII.

This system was difficult to model. In order to represent the effect of changes in emulsifier concentration on conversion and particle size evolution curves, the model required the fitting of the radius of a micelle and the emulsifier CMC. The following general trends and observations were evident for the fitted parameters:

- entry rate coefficients increase with temperature;
- surface area covered by a surfactant molecule increases with temperature and with increased methyl methacrylate content;
- glass effect parameter A_5 does not show any definite trend;

Table XI Values of Parameters Fitted for Runs 1, 2, 6, and 13 of System Methyl Methacrylate/ Vinyl Acetate (70°C)

Parameter	Value 30/70	Value 70/30	Units
rad-mic	8.5×10^{-8}		dm
$k_{m_m} = k_{m_p}$	7×10^{-5}	5.8×10^{-5}	m/s
a_{em}	1.6×10^{-18}	1.3×10^{-17}	m^2
$D_{eff,1}D_{eff,2}$	2×10^{-11}	2×10^{-11}	m^2/s
Gel effect, A_5	4.9×10^{-2}	2.2×10^{-2}	L
Gel effect, A_6	3.6×10^{-8}	4.5×10^{-4}	

- CMC of the emulsifier increases with temperature;
- effective diffusion coefficients increase with temperature for low VA content and decrease with temperature for high VA content.

The last observation can be explained in terms of the trend of VA-rich copolymers of producing significant gel (around 30–40%). At high contents of VA, higher temperatures will favor the formation of gel, which will hinder radical diffusion.

In some systems the influence of the copolymer composition on the surfactant equilibrium has been reported.[52] Also, it is interesting to mention that one of the reviewers of this paper pointed out to us that he/she has measured significant changes in the surfactant CMC value in the presence of changes in monomer composition. Also, the dependence of CMC with temperature has been reported as being rather complex, showing sometimes a maximum.[53] As for the lack of trend

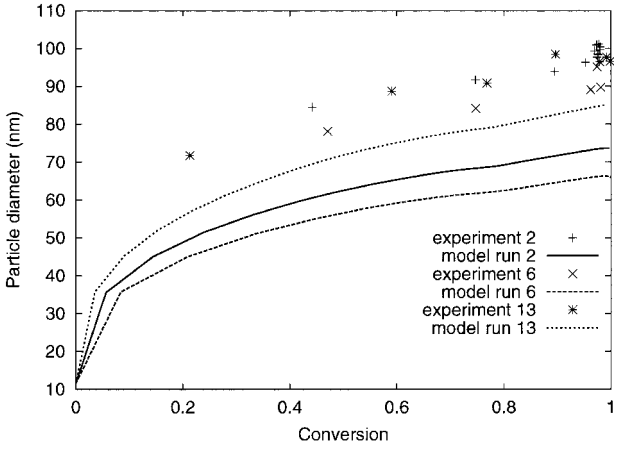

Figure 22 Model and experimental average particle diameter–conversion curves for the MMA/VA system, runs 2, 6, and 13.

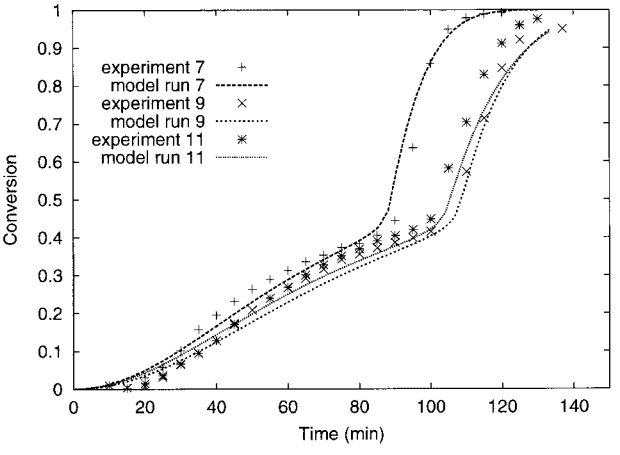

Figure 23 Model and experimental conversion–time curves for the MMA/VA system, runs 7, 9, and 11.

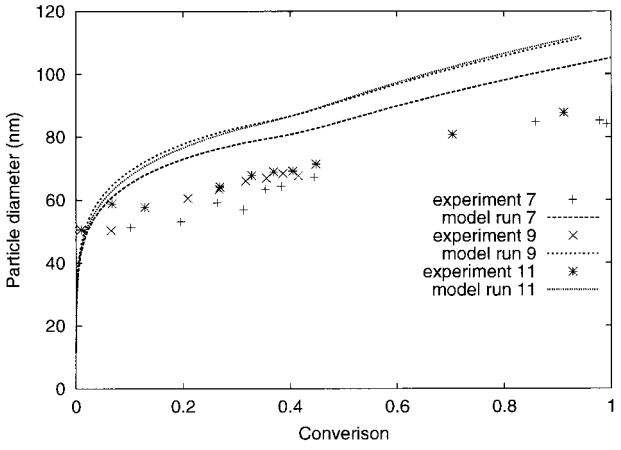

Figure 24 Model and experimental average particle diameter– conversion curves for the MMA/VA system, runs 7, 9, and 11.

shown by the glass effect parameter A_5, it is pertinent to point out that the kinetics of copolymerization of MMA/VA, even in bulk systems, is still not well understood. The complexity of this system is due to the difficulty posed by simultaneous complications in the propagation step (possible penultimate effect[25]) and the termination step (gel effect).[54]

One of the features of this system that makes the fitting of experimental data challenging is the presence of two well-defined regions in the conversion–time curves. This can be seen in Figures 19, 21, 23, and 25, and has been reported and discussed before.[8,23] The reason for this behavior is the wide difference of copolymerization reactivity ratios for MMA and VA.[55] This difficulty was evident in the fitting of conversion–time curves for runs 6 and 12. The model captures qualitatively the correct behavior but for those two runs the model overpredicts the rate of reaction, especially for the second region of the curves; the exact reason for this deviation is unknown.

Table XII Values of Parameters Fitted for Runs 7, 9, 11, and 4, 8, 12 of System Methyl Methacrylate/Vinyl Acetate (60°C)

Parameter	Value 30/70	Value 70/30	Units
rad-mic	8.5×10^{-8}	3.5×10^{-8}	dm
$k_{m_m} = k_{m_p}$	8×10^{-7}	9×10^{-7}	m/s
a_{em}	1.4×10^{-18}	2×10^{-18}	m^2
CMC	8×10^{-4}	2×10^{-4}	gmol/L
$D_{eff,1}D_{eff,2}$	4.5×10^{-11}	1.5×10^{-11}	m^2/s
Gel effect, A_5	1.5×10^{-3}	1.5×10^{-2}	L
Gel effect, A_6	5.9×10^{-1}	5.2×10^{-3}	

The phenomenon of consecutive homopolymerizations is also illustrated in Figures 26 and 27. Figure 26 shows the rate of polymerization predicted by the model for experiment 1. The curve shows two peaks corresponding to the consecutive "homopolymerizations" of BA (with a small amount of co-VA) and VA (with a small amount of co-BA). Figure 27 shows the model predictions of $\tilde{n}$-conversion curves for experiments 1 and 2. When VA polymerization becomes predominant, $\tilde{n}$ decreases due to the high transfer to monomer and desorption rate of VA radicals. The phenomena predicted by the model have also been observed by previous researcher.[8]

Another deviation of the model with respect to the experimental data is exhibited in the particle size– conversion curves for the set of runs 2, 6, and 13 and for the set of runs 7, 9, and 11. Again,

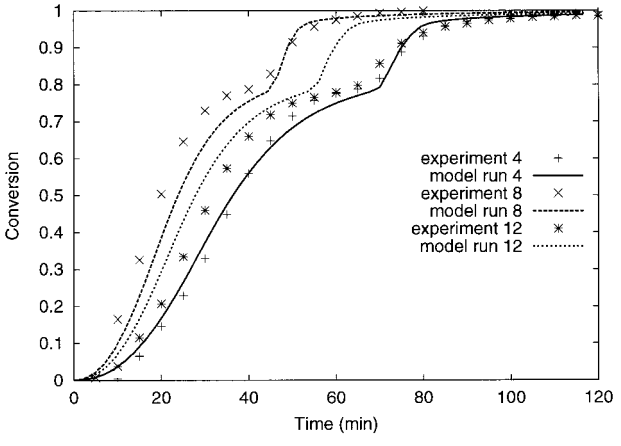

Figure 25 Model and experimental conversion–time curves for the MMA/VA system, runs 4, 8, and 12.

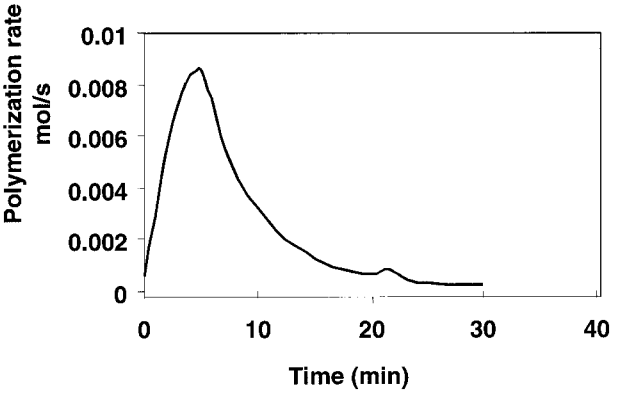

Figure 26 Polymerization rate–time curve predicted by the model for the BA/VA system, run 1.

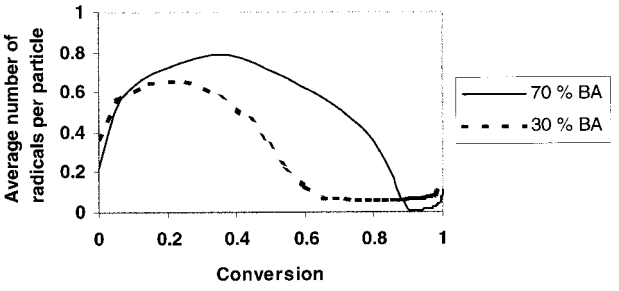

Figure 27 Average number of radicals per particle–conversion curves predicted by the model for the BA/VA system, runs 1 and 2.

the relative location of the curves is correctly predicted by the model, but for the first set the model underpredicts the values by 15–25% and for the second set the model overpredicts the values by similar percentages. The rest of the data are reasonably well fitted by the model.

System Vinyl Acetate/Butyl Acrylate

Runs 1, 5, 2, 6, and 13 were all performed at 70°C. Monomer molar ratios used were 30/70 VA/BA for runs 1, 5, and 70/30 VA/BA for runs 2, 6, and 13. Values for fitted parameters are given in Table XIII and comparison of experimental and model-predicted curves is made in Figures 28–31; they correspond to conversion–time and average particle size–conversion, respectively.

For experiments run at 60°C, two sets of data were considered for analysis: (1) runs 3, 7, and 9 with 30/70 VA/BA molar composition; and (2) runs 4, 10, and 12 with 70/30 VA/BA molar composition. Model and experimental conversion–time curves are presented in Figures 32–35 and Table XIV contains the values of fitted parameters.

General observations for adjusted parameters of this system are as follows:

Table XIII Values of Parameters Fitted for Runs 1, 5, and 2, 6, 13, of System Butyl Acrylate/Vinyl Acetate (70°C)

	Value		
Parameter	30/70	70/30	Units
$k_{m_m} = k_{m_p}$	2×10^{-6}	4×10^{-7}	m/s
a_{em}	6.5×10^{-18}	9.8×10^{-18}	m^2
$D_{eff,1}$	5×10^{-14}	2×10^{-12}	m^2/s
$D_{eff,2}$	5.6×10^{-10}	9×10^{-9}	m^2/s

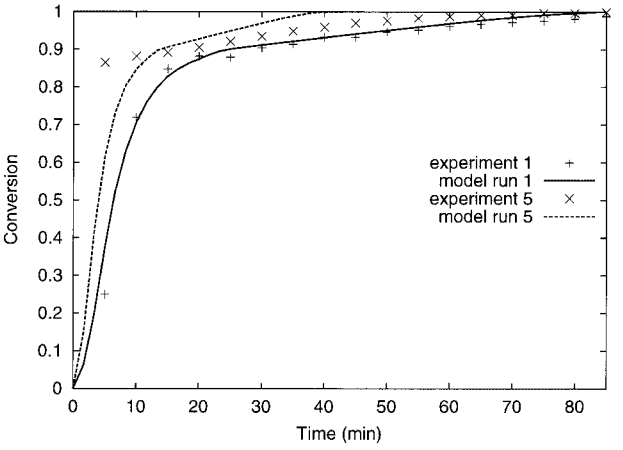

Figure 28 Model and experimental conversion–time curves for the BA/VA system, runs 1 and 5.

- entry rate coefficients increase with increased content of VA;
- surface area covered by a surfactant molecule increases with increased butyl acrylate content;
- no definite trend is observed for effective diffusion coefficients.

No gel effect correlation was used for these simulations, although there seems to be some evidence of its presence in runs 4, 10, and 12. Due to very different copolymerization reactivity ratios for this system, the curves conversion–time show a steady consumption of BA during the first stage; in this period the reaction is close to a BA homopolymerization. After most BA has been consumed, VA starts to react and the global rate of

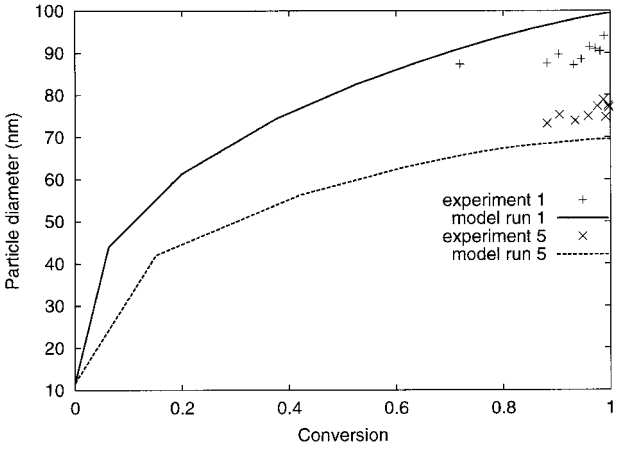

Figure 29 Model and experimental average particle diameter–conversion curves for the BA/VA system, runs 1 and 5.

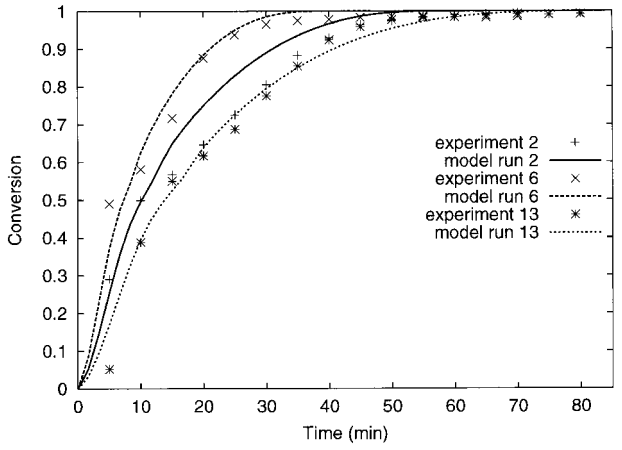

Figure 30 Model and experimental conversion–time curves for the BA/VA system, runs 2, 6, and 13.

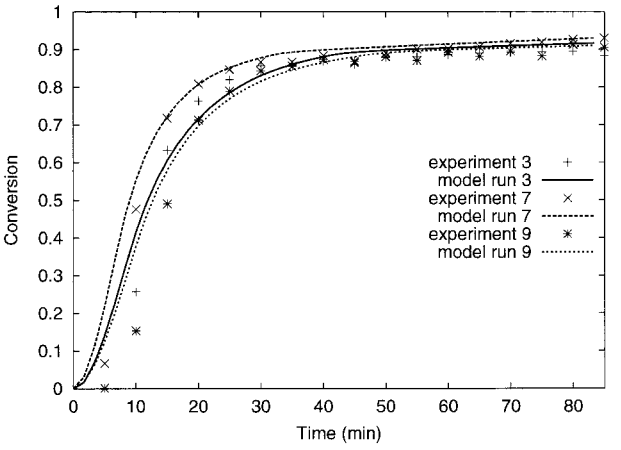

Figure 32 Model and experimental conversion–time curves for the BA/VA system, runs 3, 7, and 9.

reaction strongly decreases. This effect is well explained by the model simulations in Figure 32 in which, after 80% conversion (30/70 VA/BA molar composition), the rate of polymerization approaches zero. However, in Figure 34 the experimental curves of runs 4, 10, and 12 show a more complex behavior, and the model fitting is not good. In this case, for a molar composition of 70/30 VA/BA, after most BA has been consumed (40% conversion), the rate of reaction decreases to a lower value than the one predicted by the model, especially for runs 4 and 12, and at higher conversions a gel effect, not included in the model, seems to set on.

Model Lack of Fit for Particle Size Data

Regarding average particle size, for all the systems studied, model performance is similar to that observed for styrenic systems: lack of fit between model and experiment is still significant but the model qualitatively captures the relationship between particle size and reaction rate. Smaller particles correspond to a larger number of them and faster reaction rates. That the general trends are correctly predicted by a model that only includes the micellar nucleation mechanism points out the predominance of this nucleation mechanism over others. This confirms order of magnitude estimations,[56] which clearly indicate the predominance of micellar nucleation over homogeneous nucleation when operating above the CMC of the emulsifier. Lack of fit between model predictions and experimental data for average particle size may be explained as a consequence of the complexity of the nucleation phenomena,

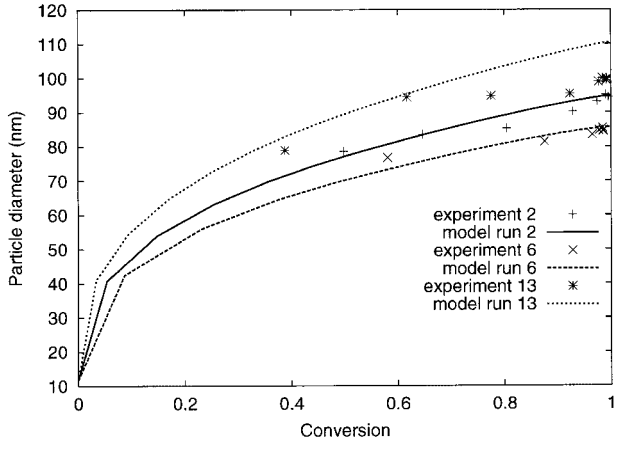

Figure 31 Model and experimental average particle diameter–conversion curves for the BA/VA system, runs 2, 6, and 13.

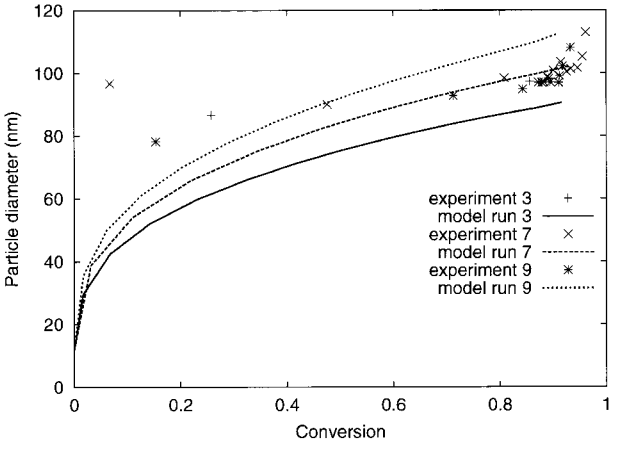

Figure 33 Model and experimental average particle diameter– conversion curves for the BA/VA system, runs 3, 7, and 9.

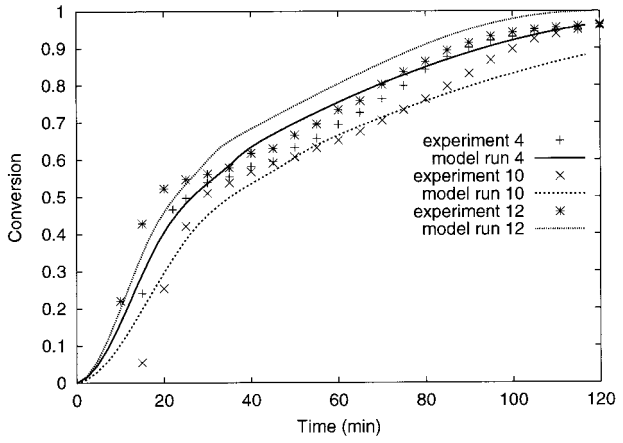

Figure 34 Model and experimental conversion–time curves for the BA/VA system, runs 4, 10, and 12.

which is still not completely understood and which may include other nucleation mechanisms. Also, the sensitivity of the nucleation phenomena to small amounts of impurities is a factor that may affect the experimental data.

CONCLUSIONS

In this paper, results of experimental data for conversion and particle size evolution, as well as comparison with model predictions, are presented for four emulsion copolymerizations containing acrylic monomers. For the first time, the applicability of a general mathematical model for emulsion copolymerization, through its ability to fit and explain experimental data of conversion, particle size, and copolymer composition, is extensively tested. The experiments covered a wide range of conditions in which variations on initiator and surfactant concentrations, water to monomer ratio, comonomer composition, and temperature were included. The aim of this work was to assess the power of the model for practical applications.

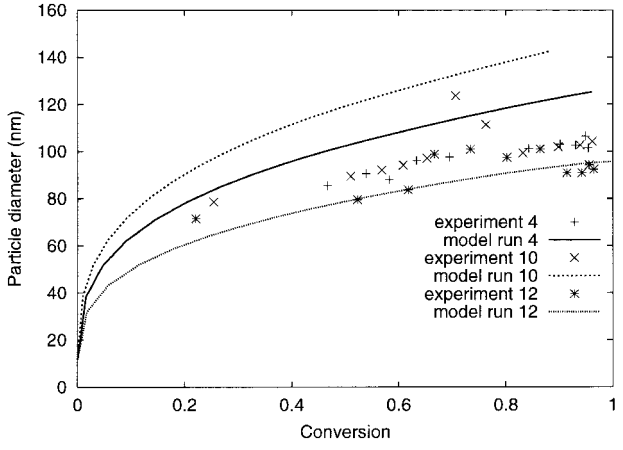

Figure 35 Model and experimental average particle diameter–conversion curves for the BA/VA system, runs 4, 10, and 12.

Table XIV Values of Parameters Fitted for Runs 3, 7, 9, and 4, 10, 12, of System Butyl Acrylate/Vinyl Acetate (60°C)

	Value		
Parameter	30/70	70/30	Units
$k_{m_m} = k_{m_p}$	1.8×10^{-7}	5×10^{-6}	m/s
a_{em}	1.5×10^{-17}	2.5×10^{-18}	m^2
$D_{eff,1}$	1×10^{-11}	2×10^{-9}	m^2/s
$D_{eff,2}$	6×10^{-9}	1.2×10^{-9}	m^2/s

As in the previous paper dealing with styrenic systems, it is worthwhile to mention that the model predicts well the evolution of copolymer composition with conversion using reactivity ratios taken from the literature. Again, for space constraints, it is not possible to include plots showing model predictions and experimental data for copolymer composition, but these plots are similar to those included in the first paper of the series[46] obtained with a simpler model.

Due to the formidable complexity of emulsion copolymerization systems, parameter fitting of unknown and uncertain parameters of the model is required to fit large sets of data. Despite all the efforts in modeling emulsion polymerization, still an important set of parameters are of semiempirical nature if a model of reasonable generality is to be written out. The approach in this work was to allow changes in adjustable parameters for a given copolymerization system, depending on temperature and initial monomer composition, but keeping the parameters constant for simultaneous variations in emulsifier concentration, initiator concentration, and monomer to water ratio. Also, values for fitted parameters were allowed to change between physically reasonable limits, based on information available in the literature from the corresponding homopolymerization systems.

Parameter estimation for these systems is also a challenging task. Large sets of data, as the ones presented in this series, as well as specialized tools of experimental design and estimation, are necessary for reliable data fitting

and parameter estimation. Some work addressing the unicity in determination of parameters is in progress.[57]

Given the complexity and peculiarities of specific emulsion copolymerization systems, the question has been raised if it is at all possible to have a general model for this type of system.[58] It is clear that we are still not able to totally achieve predictive modeling for these systems, especially due to the lack of independently measured parameters. Still, this series of papers tries to show where we stand now in terms of quantitative modeling and which areas need further research work.

It was again found, as in part 1 of this series, that several parameters, especially a_{em} and CMC of the surfactant, entry rate coefficients k_{mmi} and k_{mmR} and diffusion coefficients, may depend on copolymer composition. Independent measurement of these parameters, as a function of copolymer composition, is highly desirable.

It must be emphasized that this model should be taken with caution if is to be used for parameter estimation or if parameters estimated in this work are to be used elsewhere. Due to the global nature of the model used, values of fitted parameters are affected by other estimated parameters since they are expected to be correlated given the structure of the model (e.g., D_{effi}).

Also, given the correlation structure of the model and the fact that the parameter values were kept constant throughout the course of each specific simulated reaction, the trends shown by some of the parameters may be affected by the values of other estimated parameters. It is true that for parameters such as effective diffusion coefficients or CMC, composition drift may change the parameter values during the course of the reaction; however we decided to use a unique average constant value for each parameter throughout each simulation as a reasonable first approximation.

All this confirms the conclusion of the first paper of the series in which the importance of independently measuring the adjusted parameters is emphasized.

The authors are indebted to Prof. W. Harmon Ray and the sponsors of the University of Wisconsin Polymerization Reaction Engineering Laboratory, for permission to use experimental data obtained in their laboratory, use of the POLYRED software package, and generous financial support and hospitality during the project. The authors are also grateful for valuable comments and discussions with Prof. Ray. O. Araujo wishes

Table A.I Parameters for the System Methyl Methacrylate/Butyl Acrylate

Symbol	Parameter (Units)	Value (Ref.)	Conditions
ρ_{M}	Methyl methacrylate density (kg/L)	0.887/0.899 (59)	70°C/60°C
ρ_{BA}	Butyl acrylate density (kg/L)	0.894 (60)	25°C
E_{PM}	Methyl methacrylate propagation activation energy (kJ/mol)	18.039 (59)	
A_{PM}	Arrhenius methyl methacrylate propagation constant (cm^3/mol/s)	4.9×10^8 (59)	
k_{PBA}	Butyl acrylate propagation constant (cm^3/mol/s)	1.2×10^6 (55)	
r_{M}	Methyl methacrylate reactivity ratio	1.88 (60)	60°C
r_{BA}	Butyl acrylate reactivity ratio	0.43 (60)	60°C
E_{TM}	Methyl methacrylate termination activation energy (kJ/mol)	2.932 (59)	
A_{TM}	Arrhenius methyl methacrylate termination constant (cm^3/mol/s)	9.8×10^{10} (59)	
k_{TBA}	Butyl acrylate termination constant (cm^3/mol/s)	1.8×10^7 (60)	35°C
E_{trM}	Methyl methacrylate transfer to monomer activation energy (kJ/mol)	76.562 (59)	
A_{trM}	Arrhenius methyl methacrylate transfer to monomer constant (cm^3/mol/s)	2.3×10^{11} (59)	
E_{trBA}	Butyl acrylate transfer to monomer activation energy (kJ/mol)	64.125	
A_{trM}	Arrhenius butyl acrylate transfer to monomer constant (cm^3/mol/s)	4.3×10^{11}	
Γ_∞	Parameter surfactant adsorption isotherm, gmol/m^2	3×10^{-10} [a]	
b_{s}	Parameter surfactant adsorption isotherm, L/gmol	2×10^3 [a]	
CMC	Critical micelle concentration (gmol/l)	8×10^{-3} [a]	
A_7	Gel effect parameter, L^{-1}	3.5×10^2 [a]	

[a] Estimated from ref. 1.

Table A.II Parameters for the System Methyl Methacrylate/Butadiene

Symbol	Parameter (Units)	Value (Ref.)	Conditions
ρ_M	Methyl methacrylate density (kg/L)	0.887/0.876 (59)	70°C/80°C
ρ_B	Butadiene density (kg/L)	0.571/0.533 (61)	70°C/80°C
E_{PM}	Methyl methacrylate propagation activation energy (kJ/mol)	18.039 (59)	
A_{PM}	Arrhenius methyl methacrylate propagation constant (cm^3/mol/s)	4.9×10^8 (59)	
E_{PB}	Butadiene propagation activation energy (kJ/mol)	38.874 (50)	
A_{PB}	Arrhenius butadiene propagation constant (cm^3/mol/s)	1.2×10^{11} (50)	
r_M	Methyl methacrylate reactivity ratio	0.25 (60)	90°C
r_B	Butadiene reactivity ratio	0.75 (60)	90°C
E_{TM}	Methyl methacrylate termination activation energy (kJ/mol)	2.932 (59)	
A_{TM}	Arrhenius methyl methacrylate termination constant (cm^3/mol/s)	9.8×10^{10} (59)	
k_{TB}	Butadiene termination constant (cm^3/mol/s)	1.3×10^9 [a]	
E_{trM}	Methyl methacrylate transfer to monomer activation energy (kJ/mol)	76.562 (59)	
A_{trM}	Arrhenius methyl methacrylate transfer to monomer constant (cm^3/mol/s)	2.3×10^{11} (59)	
E_{trB}	Butadiene transfer to monomer activation energy (kJ/mol)	38.874 (55)	
A_{trB}	Arrhenius butadiene transfer to monomer constant (cm^3/mol/s)	5.9×10^7 (55)	
Γ_∞	Parameter surfactant adsorption isotherm, gmol/m^2	3×10^{-10}[a]	
b_s	Parameter surfactant adsorption isotherm, L/gmol	2×10^3 [a]	
CMC	Critical micelle concentration (gmol/L)	8×10^{-3} [a]	
A_7	Gel effect parameter, L^{-1}	3.5×10^2 [a]	

[a] Estimated from ref. 1.

Table A.III Parameters for the System Methyl Methacrylate/Vinyl Acetate

Symbol	Parameter (Units)	Value (Ref.)	Conditions
ρ_M	Methyl methacrylate density (kg/L)	0.887/0.899 (59)	70°C/60°C
ρ_{VA}	Vinyl acetate density (kg/L)	0.932 (60)	20°C
E_{PM}	Methyl methacrylate propagation activation energy (kJ/mol)	18.039 (59)	
A_{PM}	Arrhenius methyl methacrylate propagation constant (cm^3/mol/s)	4.9×10^8 (59)	
E_{PVA}	Vinyl acetate propagation activation energy (kJ/mol)	18.726 (55)	
A_{PVA}	Arrhenius vinyl acetate propagation constant (cm^3/mol/s)	2×10^9 (55)	
r_M	Methyl methacrylate reactivity ratio	26 (60)	60°C
r_{VA}	Vinyl acetate reactivity ratio	0.03 (60)	60°C
E_{TM}	Methyl methacrylate termination activation energy (kJ/mol)	2.932 (59)	
A_{TM}	Arrhenius methyl methacrylate termination constant (cm^3/mol/s)	9.8×10^{10} (59)	
E_{TVA}	Vinyl acetate termination activation energy (kJ/mol)	13.376 (55)	
A_{TVA}	Arrhenius vinyl acetate termination constant (cm^3/mol/s)	3.7×10^{12} (55)	
E_{trM}	Methyl methacrylate transfer to monomer activation energy (kJ/mol)	76.562 (59)	
A_{trM}	Arrhenius methyl methacrylate transfer to monomer constant (cm^3/mol/s)	2.3×10^{11} (59)	
E_{trVA}	Vinyl acetate transfer to monomer activation energy (kJ/mol)	18.726 (55)	
A_{trVA}	Arrhenius vinyl acetate transfer to monomer constant (cm^3/mol/s)	4.6×10^5 (55)	
Γ_∞	Parameter surfactant adsorption isotherm, gmol/m^2	3×10^{-10} [a]	
b_s	Parameter surfactant adsorption isotherm, L/gmol	2×10^3 [a]	
CMC	Critical micelle concentration (gmol/L)	8×10^{-3} [a]	
A_7	Gel effect parameter, L^{-1}	3.5×10^2 [a]	

[a] Estimated from ref. 1.

Table A.IV Parameters Taken from the Literature for the System Butyl Acrylate/Vinyl Acetate

Symbol	Parameter (Units)	Value (Ref.)	Conditions
ρ_{BA}	Butyl acrylate density (kg/L)	0.894 (60)	25°C
ρ_{VA}	Vinyl acetate density (kg/L)	0.932 (60)	20°C
k_{PBA}	Butyl acrylate propagation constant (cm^3/mol/s)	1.2×10^6 (55)	
E_{PVA}	Vinyl acetate propagation activation energy (kJ/mol)	18.726 (55)	
A_{PVA}	Arrhenius vinyl acetate propagation constant (cm^3/mol/s)	2×10^9 (55)	
r_{BA}	Butyl acrylate reactivity ratio	6.35 (55)	
r_{VA}	Vinyl acetate reactivity ratio	0.037 (55)	
k_{TBA}	Butyl acrylate termination constant (cm^3/mol/s)	1.8×10^7 (60)	35°C
E_{TVA}	Vinyl acetate termination activation energy (kJ/mol)	13.376 (55)	
A_{TVA}	Arrhenius vinyl acetate termination constant (cm^3/mol/s)	3.7×10^{12} (55)	
E_{trBA}	Butyl acrylate transfer to monomer activation energy (kJ/mol)	64.125	
A_{trBA}	Arrhenius butyl acrylate transfer to monomer constant (cm^3/mol/s)	4.3×10^{11}	
E_{trVA}	Vinyl acetate transfer to monomer activation energy (kJ/mol)	18.726 (50)	
A_{trVA}	Arrhenius vinyl acetate transfer to monomer constant (cm^3/mol/s)	4.6×10^5 (50)	
Γ_∞	Parameter surfactant adsorption isotherm, gmol/m^2	3×10^{-10} [a]	
b_s	Parameter surfactant adsorption isotherm, L/gmol	2×10^3 [a]	
CMC	Critical micelle concentration (gmol/L)	8×10^{-3} [a]	

[a] Estimated from [1].

to thank CNPq, Brasil, for financial support. E. Saldívar is also grateful to CID-GIRSA and CONACYT-MEXICO, and R. Giudici to CNPq and FAPESP, for financial support. The authors thank Dr. Charles Fry of the University of Wisconsin Chemistry Department for invaluable help in the NMR analysis of copolymer composition throughout this series of papers.

APPENDIX: PARAMETERS TAKEN FROM THE LITERATURE OR ESTIMATED *A PRIORI*

REFERENCES

1. Saldívar. E.; Araujo, O.; Giudici, R.; López-Barrón, C. J Appl Polym Sci 2001, 79, 2380.
2. Araujo, O. Ph.D. thesis (in Portuguese), Polytechnic School, University of Sao Paulo, Brazil, 1997.
3. Saldívar, E.; Ray, W. H. Ind Eng Chem Res 1997, 36(4), 1322–1336.
4. Saldívar, E.; Dafniotis, P.; Ray, W. H. J Macromol Sci-Rev Macromol Chem Phys 1998, C38(2), 205–323.
5. Emelie, B.; Pichot, C.; Guillot, J. J Makromol Chem Suppl 1985, 10/11, 43.
6. Emelie, B.; Pichot, C.; Guillot, J. Makromol Chem Macromol Chem Phys 1991, 192(7), 1629–1647.
7. Urretabizkaia, A.; Sudol, E. D.; El Aasser, M. S.; Asua, J. M. J Polym Sci Polym Chem 1993, 31(12), 2907–2913.
8. Dube, A.; Penlidis, A. J Polym Int 1995, 37, 235–248.
9. Cutting, G. R.; Tabner, B. J. Eur Polym J 1995, 31(12), 1215–1219.
10. Barton, J.; Hlouskova, Z.; Juranicova, V. Macromol Chem Phys 1992, 193, 167–177.
11. Ishida, M.; Oshima, J.; Yoshinaga, K.; Horii, F. Polymer 1999, 40(12), 3323–3329.
12. Ahn, T. O.; Hwang, T. W.; Jho, J. Y. Polymer-Korea 1997, 21(2), 289–295.
13. Pan, T. C.; Kuo, J. F.; Chen, C. Y. Polym Eng Sci 1991, 31(12), 916–923.
14. Lee, C. F.; Lin, K. R ; Chiu, W. Y. J Appl Polym Sci 1994, 51, 1621–1628.
15. Unzueta, E.; Forcada, J. Polymer 1995, 36(5), 1045–1052.
16. Unzueta, E.; Forcada, J. Polymer 1995, 36(22), 4301–4308.
17. Chern, C. S.; Hsu, H. J Appl Polym Sci 1995, 55, 571–581.
18. Shapiro, Y. Y.; Dorozova, N. P.; Mironova, N. M.; Balyberdina, T. G. J Polym Sci USSR 1981, 23(6), 1522–1529.
19. Yu, Y.; Dubois, P.; Teyssie, P.; Jerome, R. Macromolecules 1996, 29(19), 90–6099.
20. Yu, Y.; Dubois, P.; Teyssie, P.; Jerome, R. Macromolecules 1997, 30(15), 4254–4261.
21. Zhou, Q. Y.; Zhang, B. H.; Song, M. D.; He, B. L. Eur Polym J 1996, 32(9), 1145. –1150.
22. Canegallo, S.; Storti, G.; Morbidelli, M.; Carra, S. J Appl Polym Sci 1993, 47(6), 961–980.

23. Saldívar, E.; Ray, W. H. AIChE J 1997, 43(8), 2021–2033.
24. Brar, A. S.; Charan, S. Eur Polym J 1993, 29(5), 755–759.
25. Ma, Y.; Won, Y.; Kubo, K.; Fukuda, T. Macromolecules 1993, 26, 6766–6770.
26. Chujo, K.; Harada, Y.; Tokuhara, S.; Tanaka, K. J Polym Sci Polym Symp C 1969, 27, 321–332.
27. Pichot, C.; Llauro, M. F.; Pham, Q. T. J Polym Sci Polym Chem Ed 1981, 19(10), 2619–2633.
28. Canegallo, S.; Canu, P.; Morbidelli, M.; Storti, G. J Appl Polym Sci 1994, 54, 1919–1935.
29. Dimitratos, J.; El-Aasser, M. S.; Georgakis, C.; Klein, A. J Appl Polym Sci 1990, 40(5-6), 1005–1021.
30. Gugliotta, L. M.; Leiza, J. R.; Arotcarena, M.; Armitage, P. D.; Asua, J. M. Ind Eng Chem Res 1995, 34(11), 3899–3906.
31. Gugliotta, L. M.; Arotcarena, M.; Leiza, J. R.; Asua, J. M. Polymer 1995, 36(10), 2019–2023.
32. Saenz de Buruaga, I.; Echevarria, A.; Armitage, P. D.; de la Cal, J. C.; Leiza, J. R.; Asua, J. M. AIChE J 1997, 43(4), 1069–1081.
33. Saenz de Buruaga, I.; Armitage, P. D.; Leiza, J. R.; Asua, J. M. Ind Eng Chem Res 1997, 36, 4243–4254.
34. Vijayendran, B. R.; Bone, T.; Gajria, C. J Appl Polym Sci 1981, 26(4), 1351–1359.
35. Vijayendran, B. R.; Bone, T.; Sawyer, L. C. J Disp Sci Tech 1982, 3(1), 81–97.
36. El-Aasser, M. S.; Makgawinata, T.; Vanderhoff, J. W.; Pichot, C. J Polym Sci Polym Chem Ed 1983, 21(8), 2363–2382.
37. Misra, S. C.; Pichot, C.; El-Aasser, M. S.; Vanderhoff, J. W. J Polym Sci Polym Chem Ed 1983, 21(8), 2383–2396.
38. Erbil, H. Y. Polymer 1996, 37(24), 5483–5491.
39. Delgado, J.; El-Aasser, M. S.; Vanderhoff, J. W. J Polym Sci A Polym Chem 1986, 24(5), 861–874.
40. Jourdan, C.; Cavaille, J. Y.; Perez, J. Polym Eng Sci 1988, 28(20), 1318–1325.
41. Kong, X. Z.; Pichot, C.; Guillot, J. Colloid Polym Sci 1987, 265(9), 791–802.
42. Kong, X. Z.; Pichot, C.; Guillot, J.; Cavaille, J. Y. ACS Symp Ser 1992, 492, 163–187.
43. Sun, P. Q.; Liu, D. Z.; Zhao, K.; Chen, G. T. Acta Polym Sinica 5, 542–548 (1998).
44. Bataille, P.; Bourassa, H. J Polym Sci A 1988, 27(1), 357–365.
45. Abd. El-Ghaffar, M. A.; Badran, A. S.; Shendy, S. M. M. J Elastomers Plast 1992, 24(3), 192–202.
46. Araujo, O.; Giudici, R.; Saldívar, E.; Ray, W. H. J Appl Polym Sci 2001, 79, 2360.
47. Schmidt, A. D.; Ray, W. H. Chem Eng Sci 1981, 36, 1401–1410.
48. Forcada, J.; Asua, J. M. J Polym Sci Part A Polym Chem 1990, 28, 987.
49. Lovell, P. A.; Shah, T. H.; Heatley, F. Polym Comm 1991, 32(4), 98–103.
50. Odian, G. Principles of Polymerization, 3rd ed.; Wiley Interscience: New York, 1991; Chap 3.
51. Nomura, M. In Emulsion Polymerization; Piirma, I., Ed.; Academic Press: New York, 1982.
52. Özdeger, E.; Sudol, E. D.; El-Aasser, M. S.; Klein, A. J Polym Sci Part A Polym Chem 1997, 35, 3837–3846.
53. Goddard, E. D.; Ananthapadmanabhan, K. P., Eds. Interaction of Surfactants with Polymers and Proteins; CRC Press: Boca Raton, FL, 1993.
54. Pinto, J. C.; Ray, W. H. Chem Eng Sci 1995, 50, 715–736.
55. Brandrup, J.; Immergut, E. H. Polymer Handbook, 3rd ed.; Wiley Interscience: New York, 1989.
56. Herrera-Ordóñez, J.; Olayo, R. J Polym Sci Part A Polym Chem 2000, 38, 2201.
57. López-Serrano, F.; Fernández, C. R.; Puig, J. E.; Alvarez , J. Macromol Symp 2000, 150, 59–64.
58. van Herk, A. M.; German, A. L. Macromol Theor Simul 1998, 7(6), 557–565.
59. Reichert, K. H.; Moritz, H. U., Eds. 5th Workshop of Polymer Reaction Engineering; DECHEMA Monographs; VCH: New York, 1995.
60. Brandrup, J.; Immergut, E. H. Polymer Handbook, 2nd ed.; Wiley Interscience: New York, 1975.
61. Perry, R. H.; Chilton, C. H. Chemical Engineers Handbook, 5th ed., Wiley: New York, 1993.